NASA TECHNICAL MEMORANDUM

NASA TM X-1899

NASA TM X-1899



# ELECTRICAL CHARACTERISTICS OF A LARGE AREA THIN FILM CdS SOLAR CELL

*by Ernie W. Spisz and John R. Jack*

*Lewis Research Center*

*Cleveland, Ohio*

NATIONAL AERONAUTICS AND SPACE ADMINISTRATION • WASHINGTON, D. C. • OCTOBER 1969

| 1. Report No. NASA TM X-1899 | 2. Government Accession No. | 3. Recipient's Catalog No. |
|---|---|---|
| 4. Title and Subtitle<br>ELECTRICAL CHARACTERISTICS OF A LARGE AREA THIN FILM CdS SOLAR CELL | | 5. Report Date<br>October 1969<br>6. Performing Organization Code |
| 7. Author(s)<br>Ernie W. Spisz and John R. Jack | | 8. Performing Organization Report No.<br>E-5149 |
| 9. Performing Organization Name and Address<br>Lewis Research Center<br>National Aeronautics and Space Administration<br>Cleveland, Ohio 44135 | | 10. Work Unit No.<br>124-09<br>11. Contract or Grant No. |
| 12. Sponsoring Agency Name and Address<br>National Aeronautics and Space Administration<br>Washington, D. C. 20546 | | 13. Type of Report and Period Covered<br>Technical Memorandum<br>14. Sponsoring Agency Code |

15. Supplementary Notes

16. Abstract

The electrical characteristics of a large area (54.7 $cm^2$) thin film CdS solar cell were obtained over a range of temperatures and radiant intensity levels at atmospheric conditions and in an ultrahigh vacuum (UHV) simulation facility. The electrical characteristics were obtained over the temperature range from $20^o$ to $90^o$ C at radiant intensity levels of 0.014, 0.070, 0.140, and 0.245 $W/cm^2$. By applying the conventional "lumped constants" photovoltaic equation to the data, the effect of temperature on the reverse saturation current of the diode and the effect of temperature and radiant intensity level on the series resistance were determined.

| 17. Key Words *(Suggested by Author(s))* | 18. Distribution Statement<br>Unclassified - unlimited | | |
|---|---|---|---|
| 19. Security Classif. (of this report)<br>Unclassified | 20. Security Classif. (of this page)<br>Unclassified | 21. No. of Pages<br>25 | 22. Price*<br>$3.00 |

*For sale by the Clearinghouse for Federal Scientific and Technical Information
Springfield, Virginia 22151

# ELECTRICAL CHARACTERISTICS OF A LARGE AREA THIN FILM CdS SOLAR CELL

by Ernie W. Spisz and John R. Jack

Lewis Research Center

## SUMMARY

The electrical characteristics of a large area (54.7 $cm^2$) thin film cadmium sulfide solar cell were experimentally determined over a range of temperatures and simulated carbon arc radiant intensity levels at atmospheric conditions and in an ultrahigh vacuum (UHV) simulation facility. At atmospheric conditions the electrical characteristics were obtained over the temperature range from $20^o$ to $90^o$ C at radiant intensity levels of 0.014, 0.070, 0.140 and 0.245 watt per square centimeter. In the UHV simulation facility the electrical characteristics were determined at the same radiant intensity levels and over the temperature range from the equilibrium solar cell temperature corresponding to the incident radiant intensity level up to a temperature of $90^o$ C.

The short circuit current was a maximum and varied only slightly over the temperature range from $20^o$ to $60^o$ C. For temperatures greater than $60^o$ C the short circuit current decreased with increasing temperature. The open-circuit voltage decreased linearly with increasing temperature at the rate of approximately 0.0015 volt per K. For a constant radiant intensity level the conversion efficiency of the solar cell increased almost linearly with decreasing temperature. Within the temperature range from $20^o$ to $90^o$ C, the solar cell efficiency increased very slightly with increasing radiant intensity level for constant cell temperature. The efficiency of the particular cell tested was 3.5-percent at a temperature of $20^o$ C and a radiant intensity level of 0.140 watt per square centimeter. The maximum measured efficiency of the cell was 4 percent at a temperature of $-60^o$ C an intensity of 0.014 watt per square centimeter in the UHV simulation facility.

The application of the "lumped constants" photovoltaic equation to the experimental data permitted various electrical parameters of the cell to be evaluated. Of primary importance was the correlation of the reverse saturation current of the diode with temperature and the effect of cell temperature and radiant intensity level on the series resistance.

## INTRODUCTION

The manufacture of large area (54.7 $cm^2$) thin film cadmium sulfide (CdS) solar cells has progressed to the point where reproducible cells with reasonable conversion efficiencies of 4 to 6 percent can be produced (refs. 1 to 3). There are, however, still many factors to be resolved in order to understand the mechanism of CdS solar cells, the parameters that affect cell performance, and the influence environmental conditions have on the operational and reliability characteristics of the cell. References 4 to 7 report investigations of the effect of storage stability, moisture, and thermal cycling on cell performance, and reference 8 is a consideration of the effect of radiation damage. The authors of references 9 and 10 have studied the thermal radiation properties of these cells. In reference 10 the electrical characteristics at equilibrium temperatures corresponding to radiant intensities at solar distances from 1 to 5 astronomical units are determined.

This report presents an experimental investigation of the electrical characteristics of a CdS solar cell over a range of radiant intensities and solar cell temperatures at both atmospheric and high vacuum conditions. The experimental program consisted of obtaining the voltage-current characteristics of a CdS solar cell at four radiant intensity levels of approximately 0.014, 0.075, 0.140, and 0.245 watt per square centimeter for (1) a temperature range of $20^{\circ}$ to $90^{\circ}$ C on a bench setup at atmospheric conditions and (2) from equilibrium temperature corresponding to the incident radiant intensity level up to temperatures of $90^{\circ}$ C in a UHV space facility. Although the specific efficiency, current, and voltage levels obtained for the particular cell studied cannot be generalized as indicative of typical CdS solar cell performance, the trends obtained in these performance parameters with temperature and illumination should be fairly representative for cells of this type.

## SYMBOLS

| | |
|---|---|
| a | constant |
| I | current, A |
| $I_l$ | light generated current, A |
| $I_o$ | reverse saturation current, A |
| $I_{sc}$ | short circuit current, A |
| k | Boltzmann constant, $1.3805\times10^{-23}$, J/K |
| q | electron charge, $1.602\times10^{-19}$, C |

$R_s$ series resistance, ohm

$R_{sh}$ shunt resistance, ohm

T temperature, K or $^oC$

V voltage, V

$V_{oc}$ open circuit voltage, V

## EXPERIMENT

The thin film CdS solar cell studied herein is approximately a 3-inch (7.62-cm) square with an effective surface area of 54.7 square centimers. A cross section of the laminated structure of the cell is given in table I. The solar cell (which was manufactured during mid-1967) is composed of a silver Pyre-ML substrate on which thin layers of cadmium sulfide and cuprous sulfide are deposited. The current collector is chemically etched from a gold plated copper layer deposited on the cell surface. The cell is encapsulated by a Mylar top layer and an H-film bottom layer.

The electrical characteristics of the solar cell were obtained with the electrical circuit shown schematically in figure 1. Current-voltage curves were obtained with the variable loading resistor and/or the adjustable constant current power supply used as a bucking source. The four-wire electrical circuit provides a zero current (high impedance) loop for voltage measurement and a current carrying loop for cell loading and current measurement. The voltage-current characteristics of the cell were recorded on a high impedance x-y recorder.

Electrical characteristics were obtained on the bench setup shown in figure 2 and in the UHV space environment simulator shown in figure 3. The bench setup consisted of a controlled temperature brass plate on which the solar cell was firmly secured by evacuated slots on the front surface of the brass block. The temperature of the brass block (and therefore the solar cell temperature) was maintained at the desired value between $20^o$ to $90^o$ C by a controlled temperature, recirculating water supply. The UHV space environment facility consisted of a cryogenically pumped vacuum system with capability below $10^{-10}$ torr. The solar cell was mounted by carefully suspending the solar cell by four 22-gage copper wires fastened to each corner of the cell. The temperature of the solar cell was controlled at the desired temperature level by varying the intensity of an infrared bulb mounted below the solar cell.

The solar cell temperature was measured by a 30-gage copper-constantan thermocouple attached to the back surface of the solar cell.

Simulated solar radiation was provided by a 12-kilowatt high intensity carbon arc with associated collimating optics. The radiant intensity level was varied over the range

from 0.014 to 0.245 watt per square centimeter by aperatures or by fine mesh stainless-steel screens which act as a neutral density filter. The radiant intensity level was maintained at a constant level (as indicated by a calibrated silicon solar cell mounted in the test plane) by automatic control of the first objective lens. The spectral distribution of the carbon arc solar simulator as measured by a spectroradiometer is shown in figure 4. The carbon arc is a reasonable spectral match of the solar energy spectrum over the wavelength range of importance for the solar cell (i.e., 0.4 to 1.0 $\mu$m).

## TESTING PROCEDURE

Three series of tests were made on the cell in the following sequence:

(1) Series 1 - Bench test at atmospheric conditions for a radiant intensity range of 0.014 to 0.245 watt per square centimeter and solar cell temperatures from $20^{\circ}$ to $90^{\circ}$ C.

(2) Series 2 - UHV test for a radiant intensity range of 0.014 to 0.245 watt per square centimeter and solar cell temperatures from the equilibrium cell temperature corresponding to the radiant intensity level up to temperatures of $90^{\circ}$ C.

(3) Series 3 - Same as series 1.

The procedure that was followed to obtain the data was the same for the three series of runs. The radiant intensity level was established and held constant while the electrical characteristics of the solar cell were obtained at a number of different temperature levels over the desired temperature range. The intensity level was then changed, and the data gathering process was repeated over the same temperature range.

## RESULTS

The characteristic electrical curves of the thin film CdS solar cell for the three series of runs at the various radiant intensity levels and solar cell temperatures are shown in figure 5. The curves presented have been redrawn from the original x-y recorder traces. The original x-y recorder traces were quite "noisy" at short circuit current conditions and especially at the high radiant intensity levels. The noisy traces were due to the high-frequency fluctuations of the carbon arc solar simulator (see also ref. 7). For the series 2 UHV tank runs, the noise (or fluctuations) were so large at the highest intensity level (0.245 $W/cm^2$) that data could not be obtained.

The characteristic electrical curves for the CdS solar cell are similar to voltage-current curves for silicon solar cells. The knee of the CdS curve, however, is more rounded (indicating a lower efficiency) and the slope of the curve at short circuit current is greater than that for silicon solar cells. For temperatures greater than $20^{\circ}$ C both the short circuit current and open-circuit voltage decrease with increasing temperature

and the knee of the characteristic curve tends to flatten out noticeably with increasing temperature.

Figures 6 and 7 show the variation of short circuit current and open-circuit voltage with temperature for the various radiant intensity levels. The quality of the data is indicated by the scatter of the points shown in these figures. The scatter of the short circuit current data is fairly large; however, it should be recognized that the plotted points were obtained from the characteristic curves which were faired through the original noisy x-y recorder traces. Part of the scatter may be due to this fairing. The open-circuit voltage data have less scatter and are more consistent than the short circuit current data.

The solid or dashed lines in figures 6 and 7 are continuous x-y recorder curves obtained during cool down of the cell after the characteristic curves in figure 5 were obtained. (The continuous curves were obtained only when time and conditions permitted a controlled slow cool down of the solar cell.)

For temperatures between $20^{\circ}$ and $60^{\circ}$ C the short circuit current is approximately independent of temperature for the intensity range covered. At temperatures greater than $60^{\circ}$ C the effect of temperature is quite noticeable, and there is a pronounced decrease in short circuit current with increasing temperature. From the data obtained at 0.140 and 0.014 watt per square centimeter for series 1 runs, the short circuit current reaches a maximum at approximately $40^{\circ}$ C with a tendency to decrease slightly with decreasing temperature.

The open-circuit voltage curves shown in figure 7 are typically linear with the open-circuit voltage decreasing with increasing cell temperature. The rate of decrease for the bench data is approximately 0.0015 volt per degree. (This value for the open-circuit voltage temperature coefficient is the same as that recently obtained by the Boeing Company.) The UHV tank data indicate a lower open-circuit voltage coefficient of 0.0011 volt per degree.

Figures 8 and 9 show the effect of solar cell temperature and incident radiant intensity on the maximum conversion efficiency of the cell. (The location of the maximum power points on the characteristic curves are also indicated in fig. 5.) In figure 8, the efficiency of the cell for constant intensity, increases almost linearly with decreasing temperature. For the series 2 data at the lowest intensity level of 0.014 watt per square centimeter, the efficiency of the cell continually increases with decreasing temperature down to temperatures of $-60^{\circ}$ C. In figure 9, the effect of radiant intensity on efficiency for constant solar cell temperature is shown. There is scatter in the data, but there is a slight trend of increasing efficiency with increasing radiant intensity level.

The efficiency of the particular cell studied is approximately 3.5 percent at a temperature of $20^{\circ}$ C and a radiant intensity of 0.14 watt per square centimeter. The maximum measured cell efficiency was 4 percent at the equilibrium temperature ($-60^{\circ}$ C)

associated with the lowest radiant intensity of 0.014 watt per square centimeter in test 2.

## DISCUSSION

The variations in short circuit current, open-circuit voltage, and conversion efficiency with temperature and illumination level are fairly consistent between the three sets of data. However, there is a fair amount of scatter in the data. The scatter or poor repeatability of the data for the three series of runs is attributed to changes in the cell characteristics due to the environmental and test conditions to which the cell was exposed during the course of the experimental program. For example, in obtaining the series 1 data the cell was subjected to many ($\approx$25) thermal cycles with temperatures ranging from $20^{\circ}$ to $100^{\circ}$ C. In addition, the cell was exposed to high humidity conditions (these data were obtained during the summer months) for a period in excess of 2 months without special storage precautions being taken. Series 2 data were obtained at UHV conditions and many ($\approx$50) thermal cycles over the temperature range from $-150^{\circ}$ to $100^{\circ}$ C were encountered. Series 3 data were obtained with the cell again being subjected to the same conditions as encountered in series 1. References 4 to 7 indicate that environmental variations such as these may introduce changes within the cell that can affect its performance and reliability. In addition to the possible changes that may have been introduced into the cell by these environmental effects, there were experimental effects which also could contribute to the scatter in the data. The most important of these experimental effects were (1) the fluctuation of the carbon arc lamp, (2) the electrical circuit and components used to obtain the electrical characteristic curves, and (3) the measurement and control of the cell temperature.

The rapid fluctuations of the carbon arc exceeded the response of the automatically controlled zoom lens control system of the solar simulator and resulted in high frequency radiant intensity variations of the order of 3 to 5 percent. These fluctuations coupled with the electrical components used for solar cell loading resulted in noisy x-y recorder traces near the short circuit current conditions that were discussed previously. The power supply used to load the electrical circuit was a constant current type with a 1-ampere 32-volt capability. At high currents the high frequency intensity fluctuations could produce an instability in the power supply and an over-voltage of the cell. Periodic comparisons between the constant current power supply method of circuit loading and pure resistance loading or constant voltage (battery) supplies indicated close agreement over the range from open-circuit voltage to beyond the maximum power point. However, near the short circuit current condition, the resulting noise occurred with all the circuit loading methods and made comparison between the various methods impossible.

The single temperature measurement at the center of the solar cell could also intro-

duce experimental scatter into the data if the temperature over the large area cell were not uniform. Both short circuit current and open-circuit voltage are temperature dependent, and any temperature nonuniformities across the cell surface could introduce variations in the performance level between the data from the different runs. The UHV tank data were probably affected more by cell temperature nonuniformity than the bench data because of the different manner used to maintain constant cell temperature. The intensity output from the infrared bulb used in the UHV tank tests is not uniform and could introduce a nonuniform temperature distribution over the large surface area of the cell. The poor thermal conductivity of the thin film solar cell prevents any "evening out" of the temperature nonuniformities in the cell and an inaccurate measurement of the cell temperature could result from the single thermocouple reading. This effect may explain the differences noted between the open-circuit voltage temperature coefficient for the bench and UHV tank data.

## CORRELATION OF DATA BY PHOTOVOLTAIC EQUATION

It is possible to consider the data (especially the bench data of series 1 and 3) in terms of the "lumped constants" photovoltaic equation in order to obtain additional information regarding specific electrical parameters that can affect the performance of this type of thin film solar cell. Knowledge of these parameters may provide a clue as to the important effects governing the overall performance of the cell.

The "lumped constants" equation generally used to describe the characteristic curve of the photovoltaic cell is (see ref. 8)

$$I = I_o\left\{\exp\left[\frac{q}{akT}\left(V - IR_s\right)\right] - 1\right\} - I_l + \frac{V}{R_{sh}} - I\left(\frac{R_s}{R_{sh}}\right) \tag{1}$$

The simplicity and convenience of equation (1) and its generally accepted applicability justify its use to provide cell parameters that can be compared with values obtained for other cells and possibly to indicate trends in these parameters that may be of interest. However, it must be recognized that equation (1) does not necessarily describe the electrical characteristics of all cells under all conditions and may be somewhat inadequate for the large surface area CdS cell being studied (refs. 10 and 11).

The short circuit current $I_{sc}$ from equation (1) is

$$I_{sc} = I_o\left[\exp\left(\frac{q}{akT} I_{sc}R_s\right) - 1\right] - I_l - I_{sc}\left(\frac{R_s}{R_{sh}}\right) \tag{2}$$

If the terms containing series resistance are negligible, the short circuit current is approximately equal to the light generated current $I_l$ and therefore is directly proportional to the imposed radiant intensity. Figure 10 shows that for all the series runs at a cell temperature of $20^{\circ}$ C the short circuit current data are directly proportional to the radiant intensity. Similar curves are not shown for the data at temperatures greater than $20^{\circ}$ C because at the higher temperatures the short circuit current becomes significantly less than the light generated current, which indicates that the other terms in equation (2) are not negligible, and therefore that short circuit current is not proportional to the imposed radiant intensity.

From equation (1) the open-circuit voltage $V_{oc}$ is obtained from the relation

$$I_o\left[\exp\left(\frac{q}{akT}V_{oc}\right) - 1\right] - I_l + \frac{V_{oc}}{R_{sh}} = 0 \tag{3}$$

For a large shunt resistance $R_{sh}$ and for $I_l >> I_o$ (which is the case at the radiant intensity levels considered), equation (3) can be approximated by

$$V_{oc} \approx \frac{1}{\frac{q}{akT}} \ln \frac{I_l}{I_o} \tag{4}$$

Thus, the open-circuit voltage is linearly related to the logarithm of the light generated current (or radiant intensity) for constant cell temperature if the parameters a and $I_o$ are independent of the radiant intensity. Figure 11 shows the variation of open-circuit voltage with the radiant intensity for a cell temperature of $20^{\circ}$ C. There is some scatter in the data for the three series of runs but the accepted trend predicted by equation (4) is evident from the data.

Subtracting equation (3) from equation (2) results in the relation between short circuit current and open-circuit voltage

$$I_{sc} = I_o\left(\exp -\frac{q}{akT} I_{sc}R_s - \exp \frac{q}{akT} V_{oc}\right) - \frac{I_{sc}R_s + V_{oc}}{R_{sh}} \tag{5}$$

Equation (5) is useful because it is not necessary to assume that $|I_{sc}| \approx |I_l|$. For a cell with low series resistance and high shunt resistance, equation (5) can be approximated by

$$I_{sc} \approx -I_o \exp \frac{q}{ak} \frac{V_{oc}}{T} \tag{6}$$

Figure 12 shows the variation of short circuit current with the parameter $V_{oc}/T$. The lines of constant slope drawn through both the series 1 and 3 data predict a constant value of $q/ak$ of 12 000 for temperatures between $20^{o}$ to $90^{o}$ C. The corresponding value of the constant a is 0.968. The lines of constant slope correlate the data for both series 1 and 3 data reasonably well over this temperature range. The data for the UHV series 2 runs are not shown in figure 12 because the data for unknown reasons do not correlate by this procedure. Based on the correlation of the data in figures 10 to 12, it is possible to conclude that the assumption regarding a low series resistance and a high shunt resistance are probably reasonable.

Values of $I_o$ for each temperature can be obtained from figure 12 and are shown in figure 13 for both series 1 and 3 data. The data for both runs are correlated by the relation

$$I_o = 0.7\times10^{-21}e^{0.1T} \tag{7}$$

The effect of temperature on $I_o$ is quite pronounced. A temperature change of $20^{o}$ C results in an order of magnitude change in $I_o$. The sensitivity of $I_o$ to temperature may account for part of the scatter in the data and also for the lack of correlation of the UHV tank data with the bench data. The method of controlling the solar cell temperature in the tank with the infrared bulb could result in a nonuniform temperature distribution over the cell surface that would influence $I_o$ and correspondingly the cell output.

The series resistance of the solar cell can be approximated by the slope of the voltage-current curve at open circuit voltage (ref. 12). This slope as obtained from equation (1) is

$$\left(\frac{dI}{dV}\right)_{V_{oc}} = \frac{I_o \frac{q}{akT} \exp\frac{q}{akT} V_{oc} + \frac{1}{R_{sh}}}{1 + \frac{R_s}{R_{sh}} + I_o \frac{q}{akT} R_s \exp\frac{q}{akT} V_{oc}} \tag{8}$$

and the resulting relation for the series resistance is

$$R_s \approx \frac{1}{\left(\frac{dI}{dV}\right)_{V_{oc}}} - \frac{1}{I_o \frac{q}{akT} \exp\left(\frac{q}{akT} V_{oc}\right) + \frac{1}{R_{sh}}} \tag{9}$$

The effect of the shunt resistance term on the calculated series resistance value in equation (9) is estimated to be less than 5 percent at low radiant intensity levels and much

less than 5 percent at the high radiant intensity levels. The series resistance values calculated by equation (9) neglecting the shunt resistance term are shown in figure 14. At a temperature of $20^{\circ}$ C and a radiant intensity of 0.145 watt per square centimeter series resistance values of 0.035 and 0.068 ohm for the series 1 and 3 data compare favorably with the value of 0.05 ohm obtained on a similar solar cell in reference 3. This low value of series resistance is consistent with the assumptions made to obtain the relations used to calculate the experimental values. At low radiant intensities, however, the series resistance values are of the order of 1 ohm and the approximation may be questionable.

The increase in series resistance with decreasing radiant intensity and increasing temperature has been discussed in references 11 and 12. The magnitude of the increase for this cell, however, was much higher than expected. The series resistance is almost directly proportional to the radiant intensity. The more conventional method of determining series resistance by considering the voltage-current curve at two intensity levels (ref. 11) may be somewhat questionable especially if the two intensities are significantly different.

Comparison of the calculated series resistance values for the two series of runs in figure 14 indicates that the trends with temperature and intensity are similar but that there are differences in the absolute value of the series resistance. Whether this difference can be attributed to experimental error or an actual change in the cell resistance cannot be determined. However, if a change in cell resistance did occur, it could easily account for the scatter in the data of the various runs.

The series resistance values were not determined for the UHV series 2 runs because the correlations for a and $I_o$ could not be obtained. A comparison of the series resistance between UHV facility and bench data would have been interesting and may have shed light on whether vacuum conditions would effect this type of thin film solar cell.

Shunt resistance values could not be obtained from these data. The method of determining the shunt resistance from the slope of the voltage-current curve at short circuit current could not be used because of the noisy traces that were obtained. Although the preceding correlations suggest that the cell had a reasonably large shunt resistance; the validity of this approximation cannot be verified.

The validity of the values obtained for a, $I_o$, and $R_s$ can be qualitatively evaluated by a comparison between a calculated voltage-current curve and an experimentally obtained curve. Figure 15 shows such a comparison for the series 3 data at radiant intensities and cell temperatures of 0.14 watt per square centimeter and $20^{\circ}$ C, 0.14 watt per square centimeter and $80^{\circ}$ C, and 0.014 watt per square centimeter and $20^{\circ}$ C. The values of shunt resistance and light generated current were arbitrarily selected to pro-

vide a best fit for the data. The comparison in figure 15 is not exact but fair agreement is obtained indicating that the experimental values of a, $I_o$, and $R_s$ are reasonable.

## SUMMARY OF RESULTS

The electrical characteristics of a large area, thin film cadmium sulfide solar cell were determined. Performance data were obtained on a bench setup at atmospheric conditions and in an UHV facility for simulated radiant intensity levels of 0.014 to 0.245 watt per square centimeter and solar cell temperatures from $20^{\circ}$ to $90^{\circ}$ C. The significant results obtained were

1. The short circuit current was independent of solar cell temperature over the temperature range from $20^{\circ}$ to $60^{\circ}$ C. For temperatures greater than $60^{\circ}$ C the short circuit current decreased with increasing temperature.

2. The open-circuit voltage decreased linearly with increasing temperature at the rate of approximately 0.0015 volt per K.

3. The conversion efficiency of the cell increased almost linearly with decreasing temperature for constant radiant intensity level. For constant temperature the conversion efficiency increased slightly with increasing radiant intensity.

4. The conversion efficiency of the test cell was 3.5 percent at a temperature of $20^{\circ}$ C and an intensity of 0.140 watt per square centimeter. The maximum efficiency attained was 4 percent at a temperature of $-60^{\circ}$ C and an intensity of 0.014 watt per square centimeter in the ultrahigh vacuum simulation facility.

The experimental data were considered further in terms of the "lumped constants" photovoltaic equation with the following results:

5. The reverse saturation current of the diode could be correlated with the cell temperature. The effect of temperature was quite significant with a $20^{\circ}$ C increase in cell temperature resulting in an order of magnitude increase in reverse saturation current.

6. The series resistance of the cell increased with an increase in cell temperature and also increased very significantly with a decrease in radiant intensity level. The series resistance of the cell was quite low (0.036 and 0.068 ohm) for the two sets of bench data at a temperature of $20^{\circ}$ C and an intensity of 0.140 watt per square centimeter. The series resistance, however, increased to greater than 1 ohm at temperatures greater than $80^{\circ}$ C and a radiant intensity of 0.014 watt per square centimeter.

Lewis Research Center,
National Aeronautics and Space Administration,
Cleveland, Ohio, July 17, 1969,
124-09.

## REFERENCES


1. Shirland, F. A.; and Hietanen, J. R.: The Thin Film CdS Solar Cell. Proceedings of the Fifth Photovoltaic Specialists Conference. Vol. II. Rep. PIC-SOL-209/6, Power Information Center, Pennsylvania Univ., Jan. 1966, Paper C-3.

2. Shirland, F. A.; and Augustine, F.: Thin Film Plastic Substrate CdS Solar Cells. Proceedings of the Fifth Photovoltaic Specialists Conference. Vol. II. Rep. PIC-SOL-209/6, Power Information Center, Pennsylvania Univ., Jan. 1966, paper C-4.

3. Hietanen, J. R.; and Shirland, F. A.: The Status of the Clevite CdS Thin Film Solar Cell. Conference Record of the Sixth Photovoltaic Specialists Conference. Vol. I. IEEE, 1967, pp. 179-187.

4. Spakowski, Adolph E.; Acampora, Ferdinand L.; and Hart, Russell E., Jr.: Effect of Moisture on Cadmium Sulfide Solar Cells. NASA TN D-3663, 1966.

5. Ewashinka, John G.; and Stephenson, George K., Jr.: Thermal Cycling and Heat Damage Tests of Thin-Film Cadmium Sulfide Solar Cells. NASA TN D-3038, 1965.

6. Spakowski, Adolph E.; and Ewashinka, John G.: Thermal Cycling of Thin-Film Cadmium Sulfide Solar Cells. NASA TN D-3556, 1966.

7. Kennerud, K. L.: Simulated Space Environmental Tests on Cadmium Sulfide Solar Cells. Rep. D2-121002-1, Boeing Co. (NASA CR-72507), Feb. 28, 1969.

8. Brandhorst, Henry W., Jr.; and Hart, Russell E., Jr.: Radiation Damage to Cadmium Sulfide Solar Cells. NASA TN D-2932, 1965.

9. Liebert, Curt H.; and Hibbard, Robert R.: Theoretical Temperatures of Thin-Film Solar Cells in Earth Orbit. NASA TN D-4331, 1968.

10. Jack, John R.; and Spisz, Ernie W.: Thermal Radiative and Electrical Properties of a Cadmium Sulfide Solar Cell at Low Solar Intensities and Temperatures. NASA TN D-4818, 1968.

11. Wolf, Martin; and Rauschenbach, Hans: Series Resistance Effects on Solar Cell Measurements. Adv. Energy Conversion, vol. 3, no. 2, Apr-June 1963, pp. 455-479.

12. Schoffer, P.; and Beckman, W. A.: Evaluation of a Distributed Model of a Photovoltaic Cell. Conference Record of the Sixth Photovoltaic Specialists Conference. Vol. I. IEEE, 1967, pp. 51-69.

TABLE I. - CONSTRUCTION OF THIN FILM

CdS SOLAR CELL

| Components (front to back) | Approximate thickness, mm |
|---|---|
| Mylar | 0.025 |
| Epoxy cement | ----- |
| Gold plated copper grid | .010 |
| Cuprous sulfide | .001 |
| Cadmium sulfide | .025 |
| Zinc | .001 |
| Substrate of silver pyre ML coated on H film | .050 |

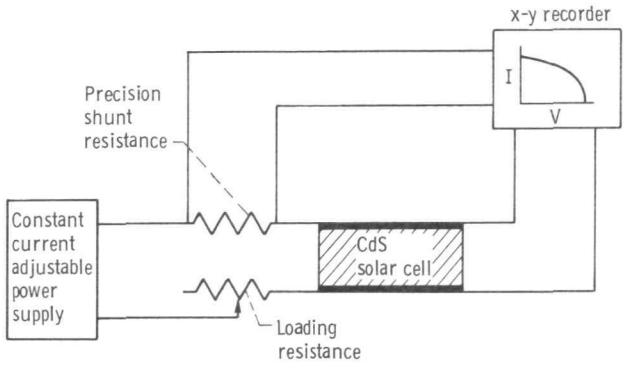


Figure 1. - Electrical schematic of four-wire circuit used for cell characteristics.

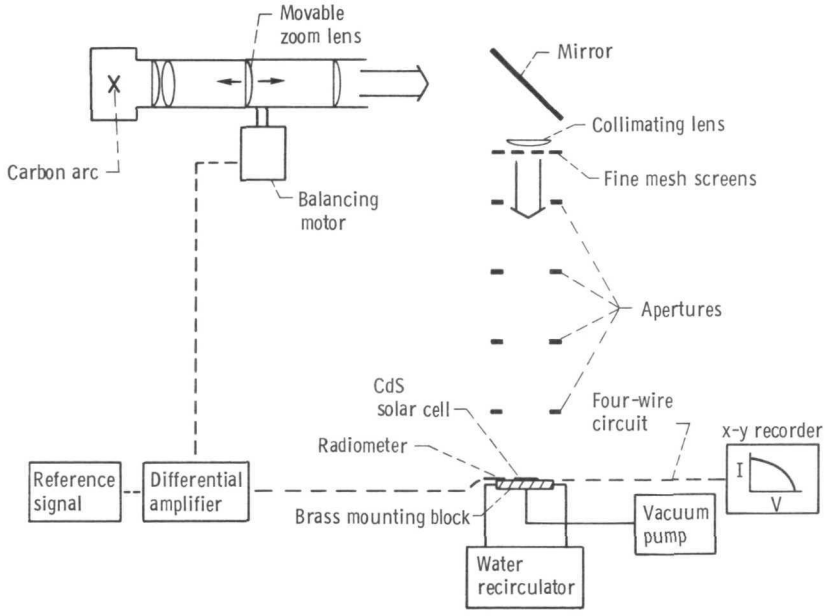


Figure 2. - Schematic drawing of bench set-up.

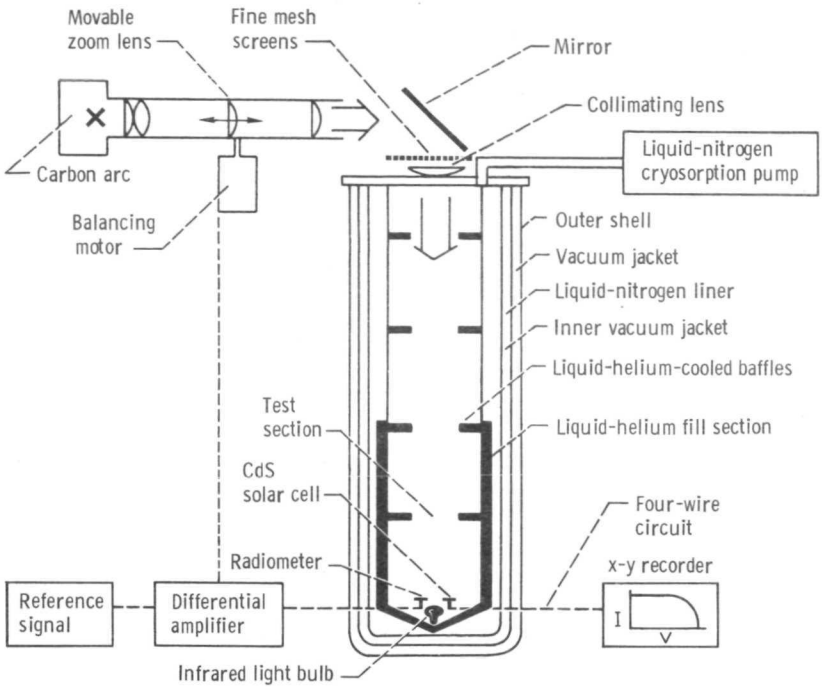


Figure 3. - Schematic drawing of high vacuum facility set-up.

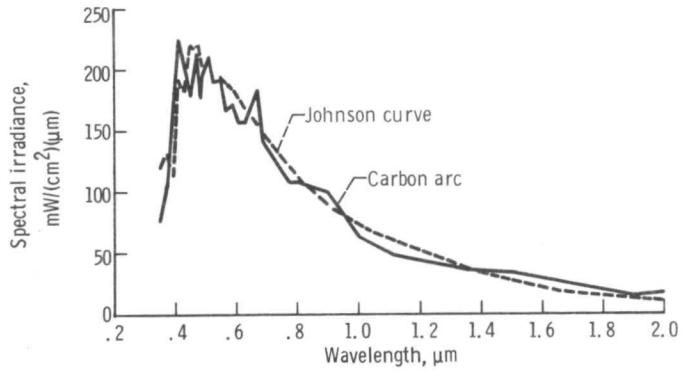


Figure 4. - Spectral irradiance of carbon arc solar simulator.

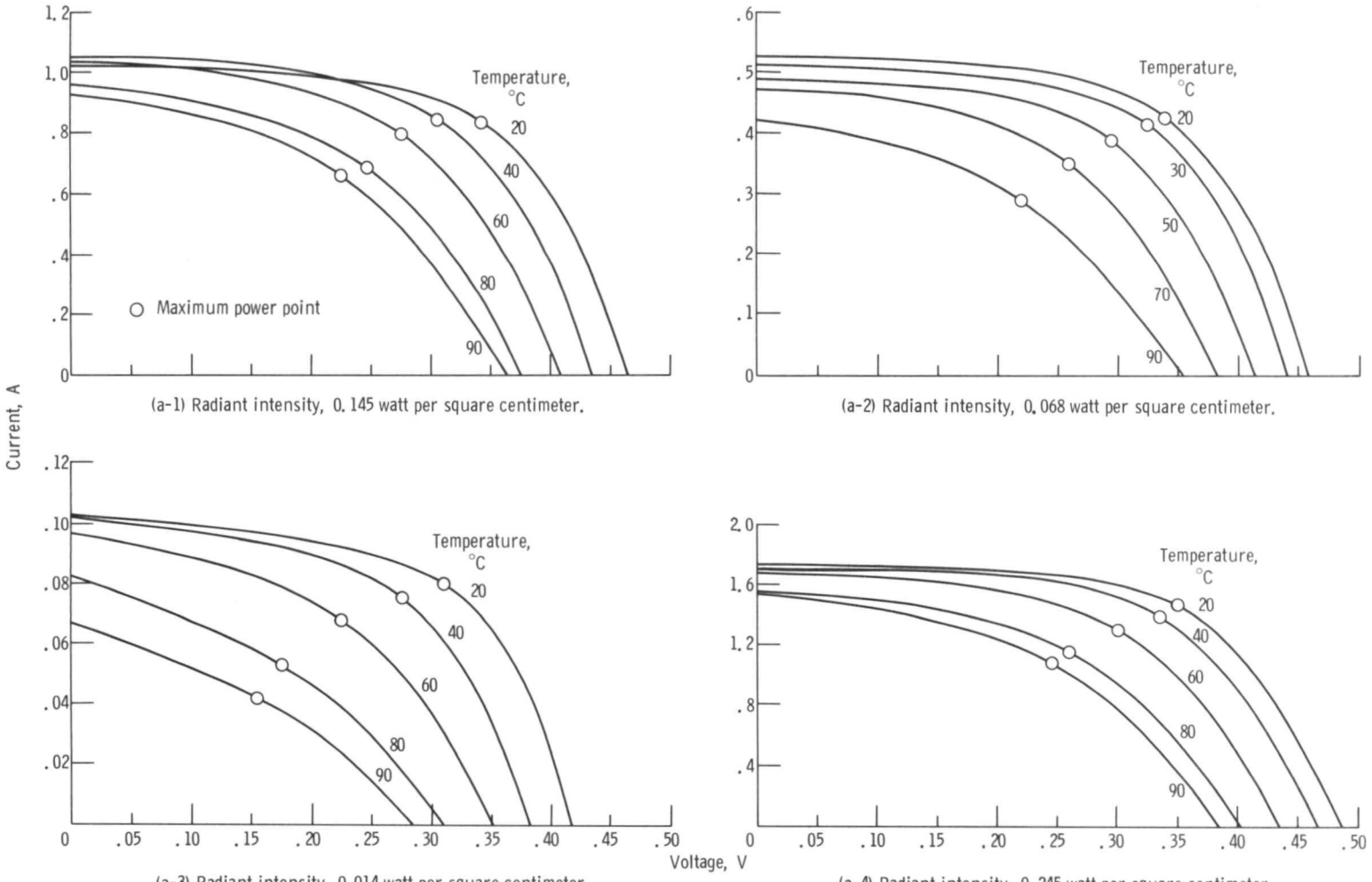


(a-1) Radiant intensity, 0.145 watt per square centimeter.

(a-2) Radiant intensity, 0.068 watt per square centimeter.

(a-3) Radiant intensity, 0.014 watt per square centimeter.

(a-4) Radiant intensity, 0.245 watt per square centimeter.

(a) Series 1; bench data.

Figure 5. - Voltage-current characteristics.

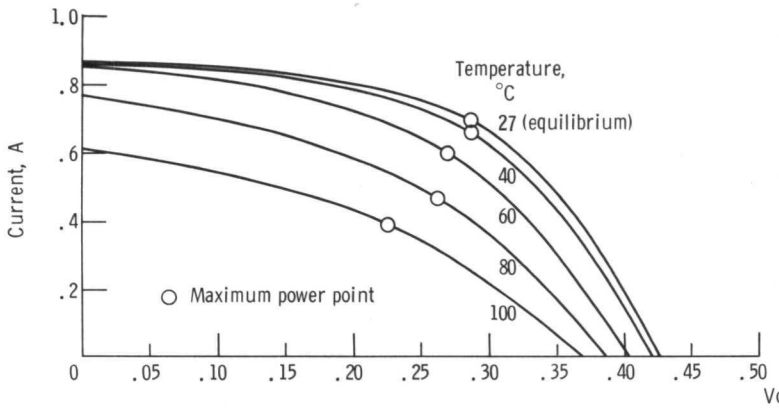


(b-1) Radiant intensity, 0.145 watt per square centimeter.

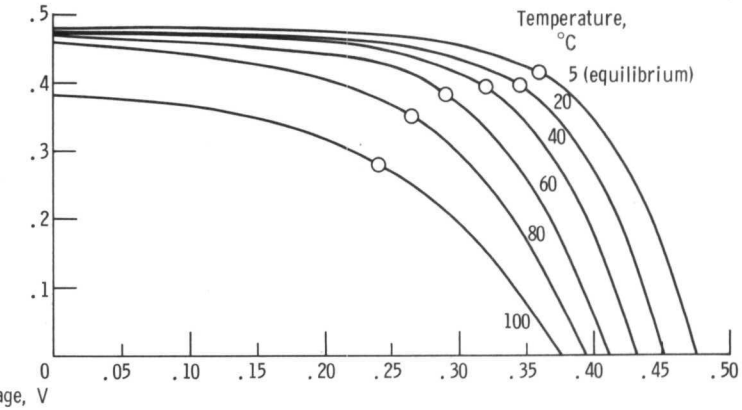


(b-2) Radiant intensity, 0.072 watt per square centimeter.

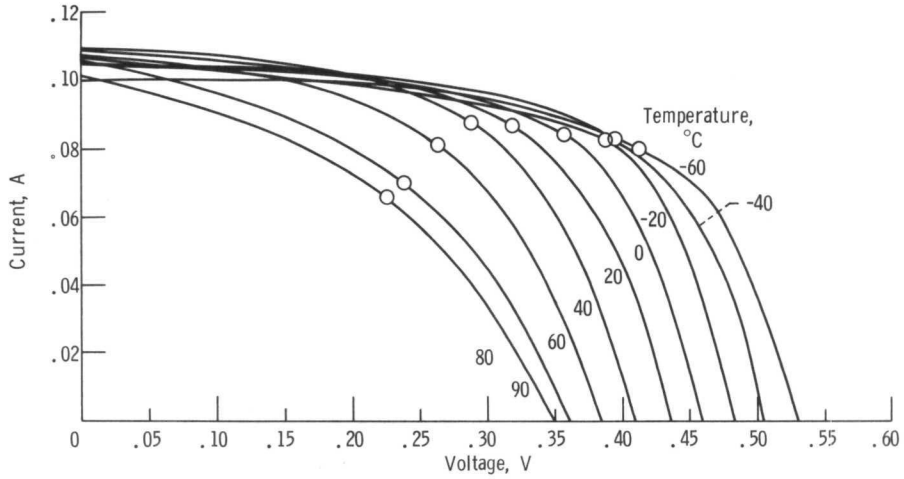


(b-3) Radiant intensity, 0.015 watt per square centimeter.

(b) Series 2; ultrahigh vacuum data.

Figure 5. - Continued.

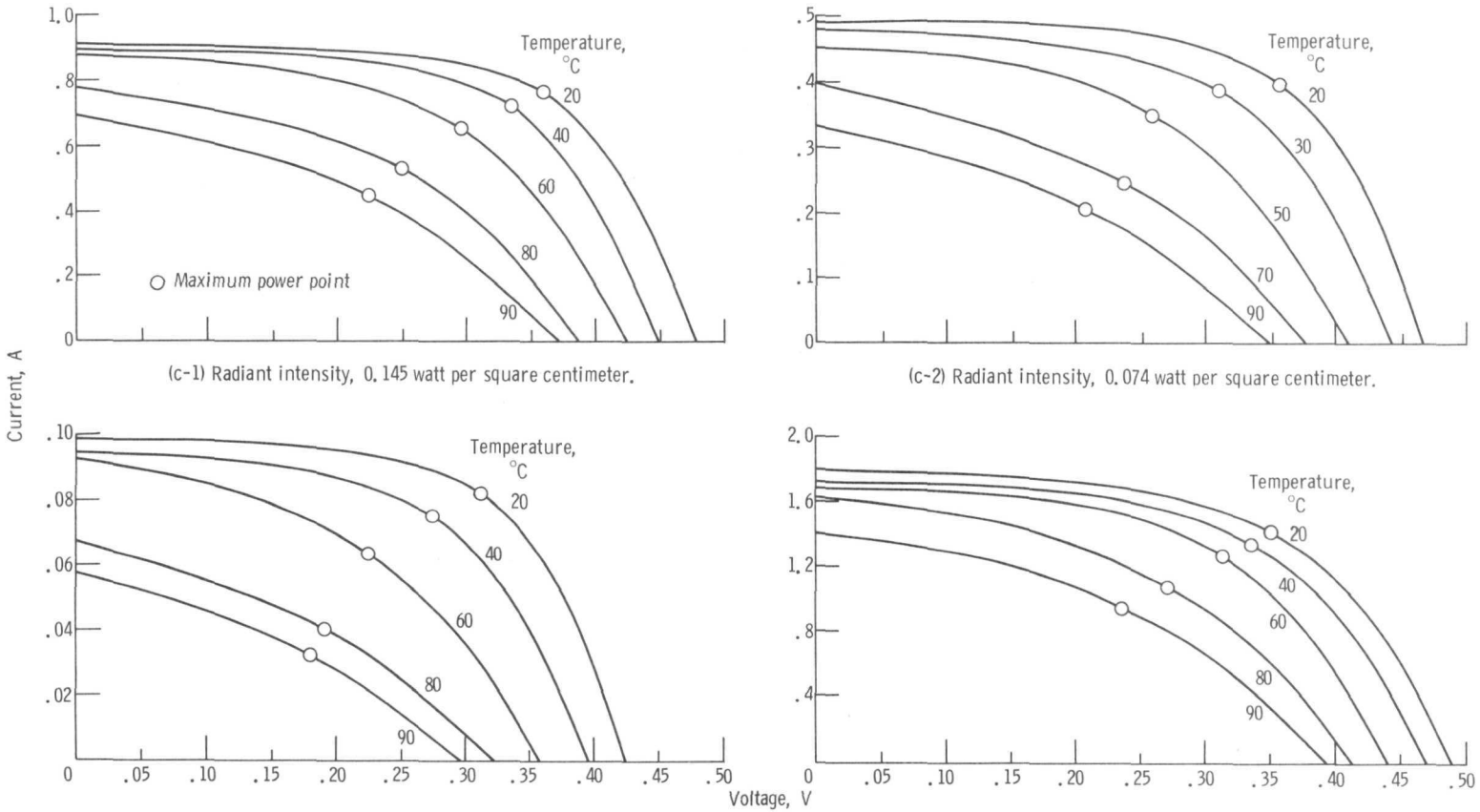


(c-1) Radiant intensity, 0.145 watt per square centimeter.

(c-2) Radiant intensity, 0.074 watt per square centimeter.

(c-3) Radiant intensity, 0.014 watt per square centimeter.

(c-4) Radiant intensity, 0.245 watt per square centimeter.

(c) Series 3; bench data.

Figure 5. - Concluded.

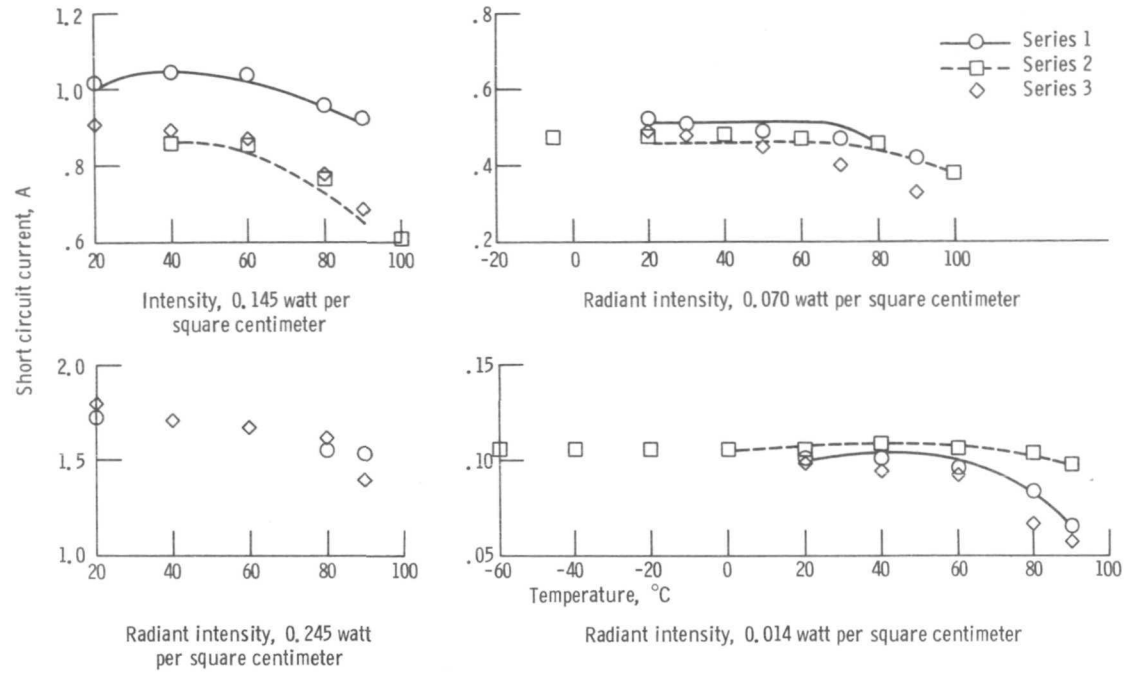


Figure 6. - Effect of temperature on short circuit current.

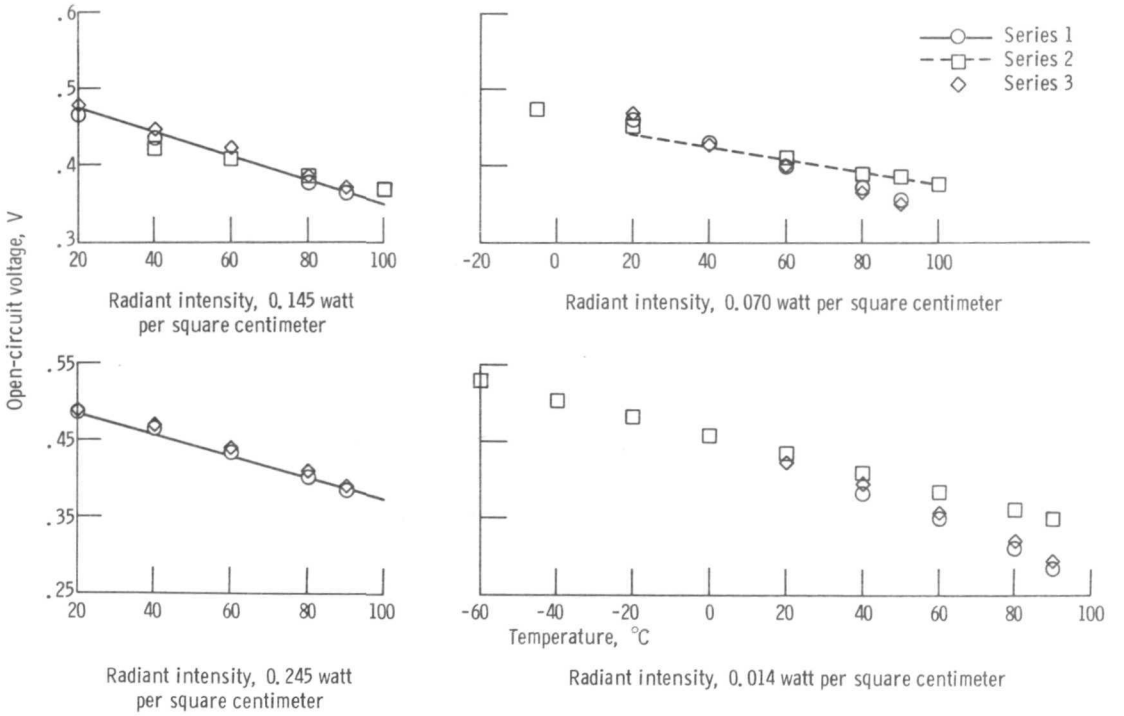


Figure 7. - Effect of temperature on open-circuit voltage.

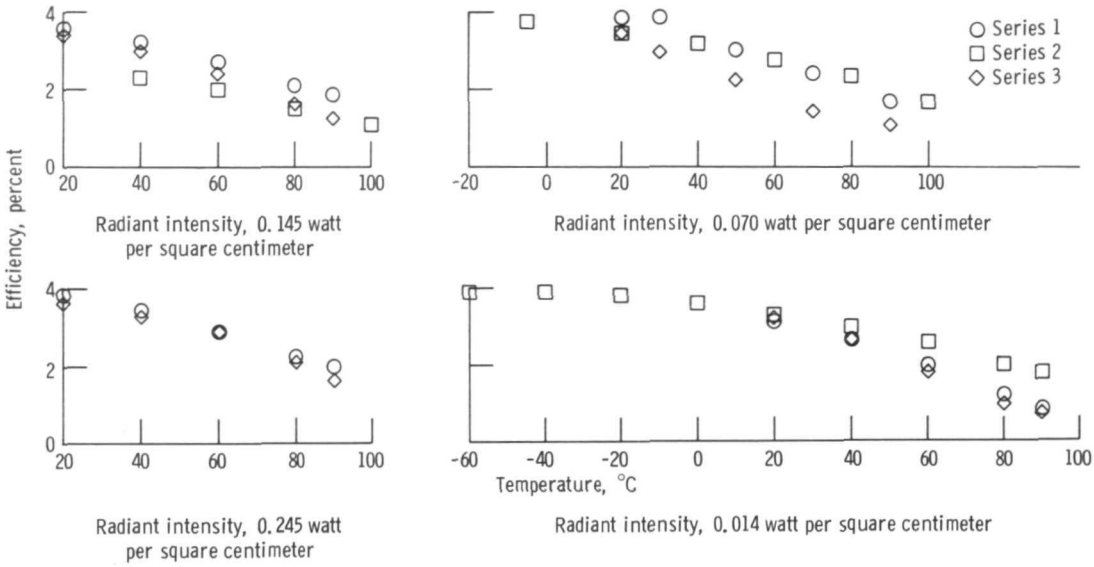


Figure 8. - Effect of temperature on cell efficiency.

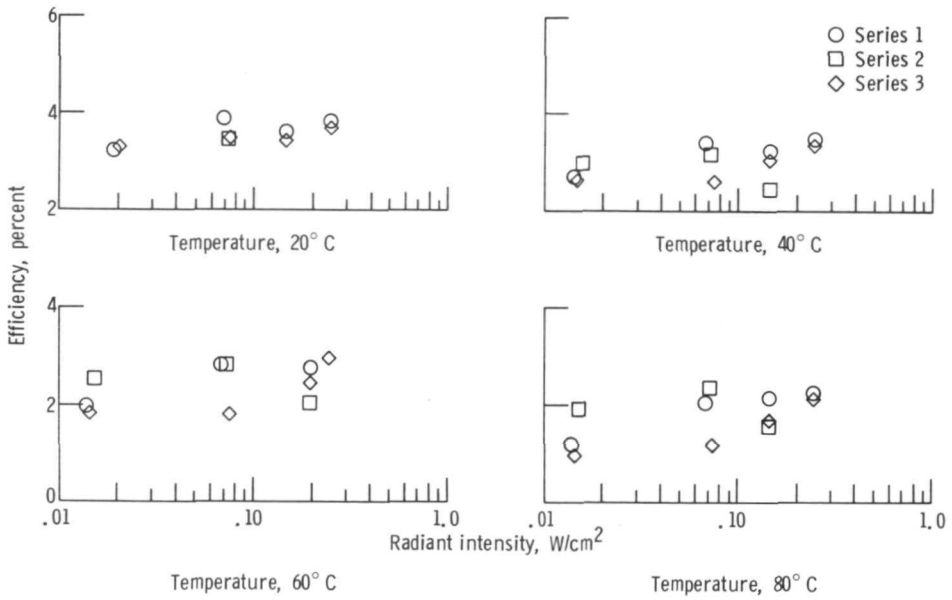


Figure 9. - Effect of intensity on cell efficiency.

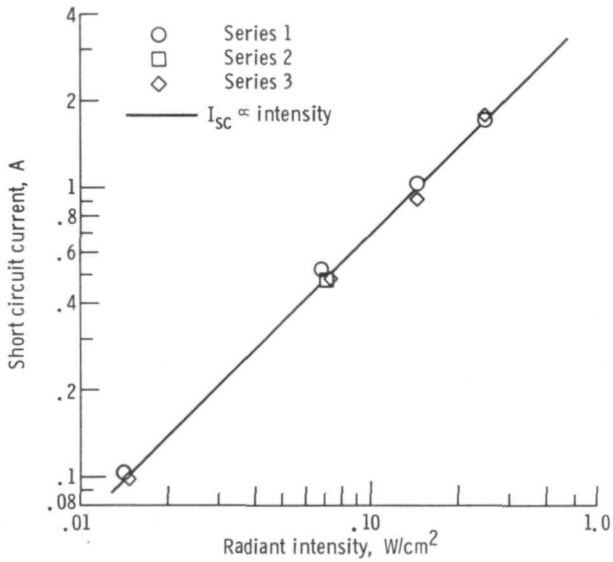


Figure 10. - Short circuit current variation with radiant intensity. Cell temperature, 20° C.

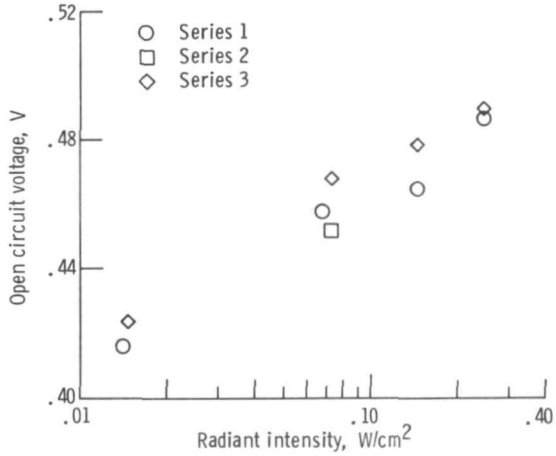


Figure 11. - Variation of open-circuit voltage with radiant intensity.

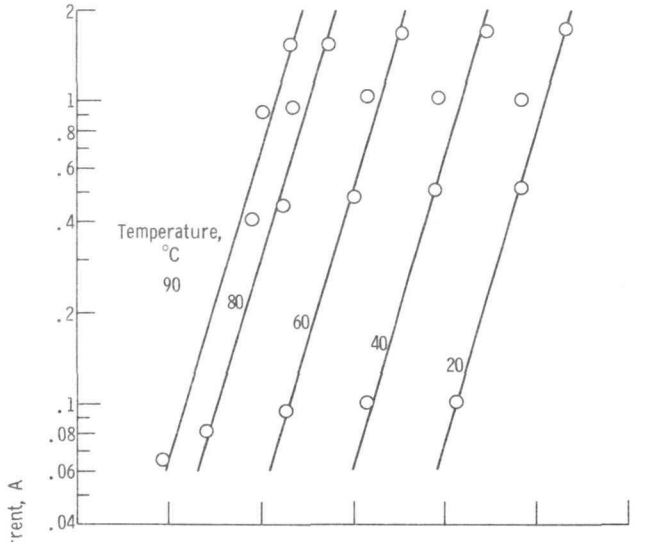


(a) Series 1 data.

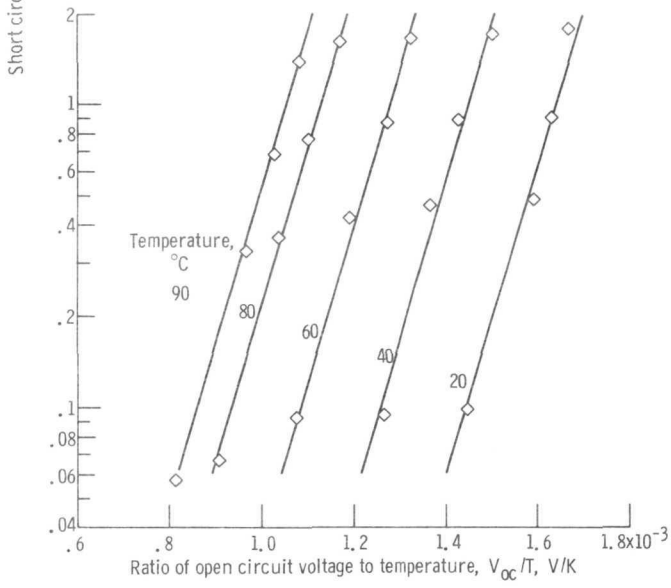


(b) Series 3 data.

Figure 12. - Short-circuit-current - open-circuit-voltage correlation.

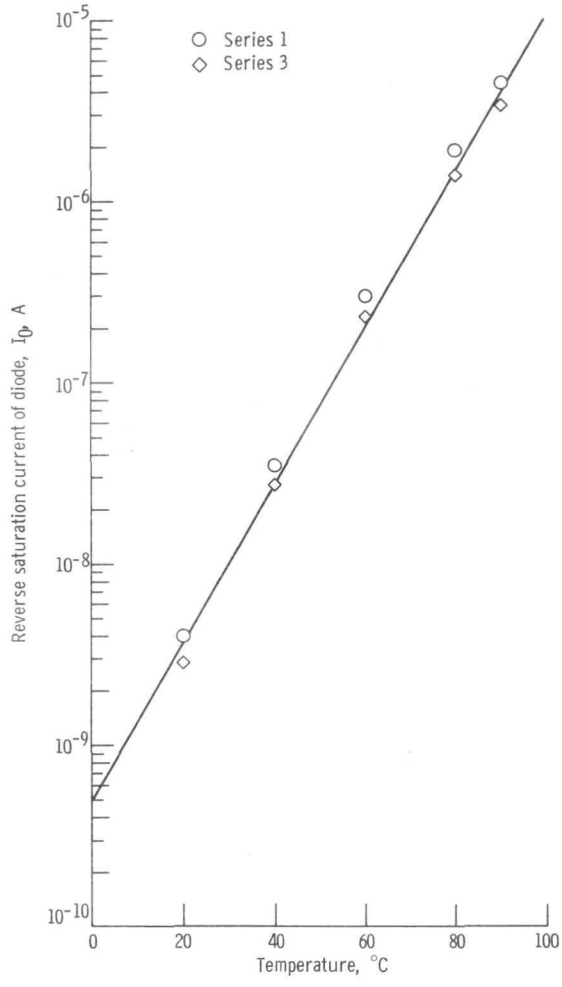


Figure 13. - Correlation of reverse saturation current of diode with temperature.

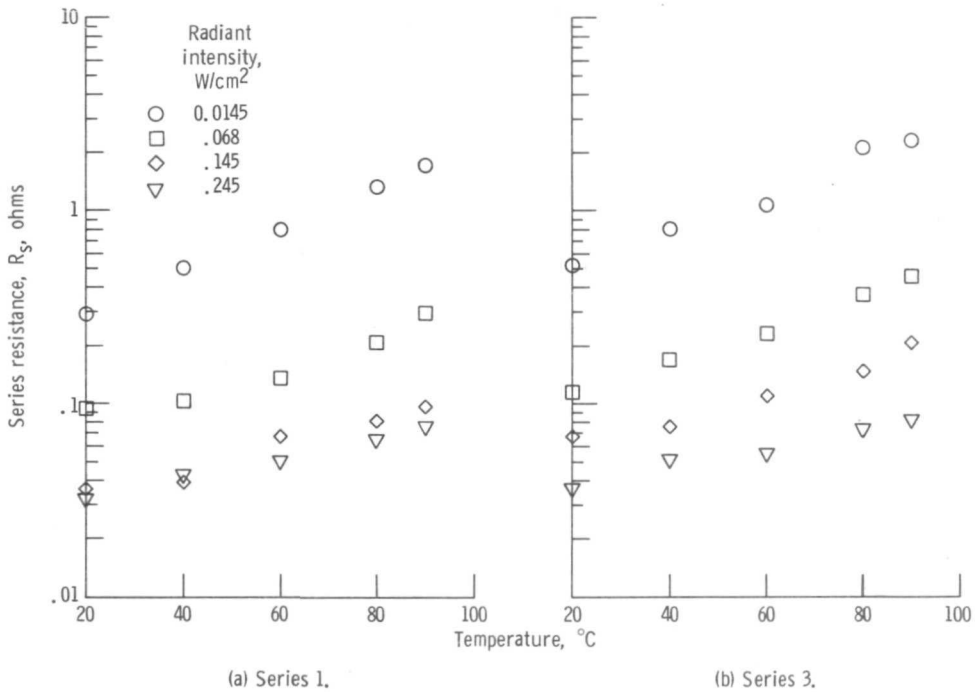


(a) Series 1. (b) Series 3.

Figure 14. - Effect of temperature and radiant intensity level on series resistance.

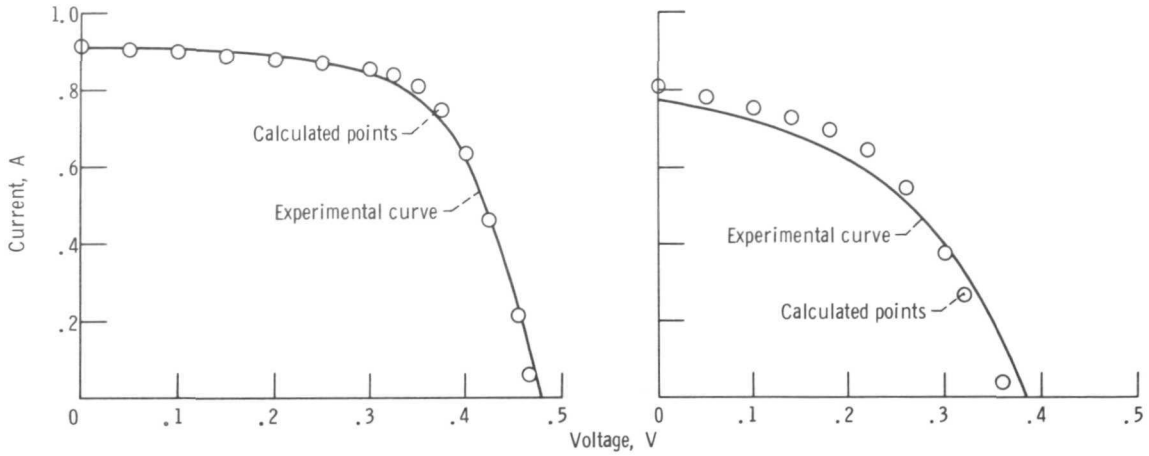


(a) Temperature, 20° C; radiant intensity, 0.145 watts per square centimeter. Points calculated for $q/akT = 40.9$; reverse saturation current, $2.89 \times 10^{-9}$ ampere; series resistance, 0.0684 ohm; shunt resistance, 5 ohms; light generated current, 0.98 ampere.

(b) Temperature, 80° C; radiant intensity, 0.145 watts per square centimeter. Points calculated for $q/akT = 34.05$; reverse saturation current, $1.40 \times 10^{-6}$ ampere; series resistance, 0.149 ohm; shunt resistance, 1.67 ohm; light generated current, 0.88 ampere.

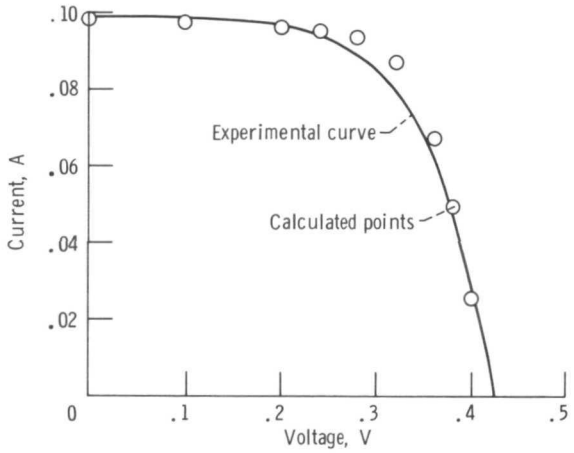


(c) Temperature, 20° C; radiant intensity, 0.014 watts per square centimeter. Points calculated for $q/akT = 40.9$; reverse saturation current, $2.89 \times 10^{-9}$ ampere; series resistance, 0.526 ohm; shunt resistance, 100 ohms; light generated current, 0.099 ampere.

Figure 15. - Comparison of measured and calculated electrical characteristic curves. Series 3 data.



NASA-Langley, 1969 — 3 E-5149

*"The aeronautical and space activities of the United States shall be conducted so as to contribute . . . to the expansion of human knowledge of phenomena in the atmosphere and space. The Administration shall provide for the widest practicable and appropriate dissemination of information concerning its activities and the results thereof."*

—NATIONAL AERONAUTICS AND SPACE ACT OF 1958

# NASA SCIENTIFIC AND TECHNICAL PUBLICATIONS

TECHNICAL REPORTS: Scientific and technical information considered important, complete, and a lasting contribution to existing knowledge.

TECHNICAL NOTES: Information less broad in scope but nevertheless of importance as a contribution to existing knowledge.

TECHNICAL MEMORANDUMS: Information receiving limited distribution because of preliminary data, security classification, or other reasons.

CONTRACTOR REPORTS: Scientific and technical information generated under a NASA contract or grant and considered an important contribution to existing knowledge.

TECHNICAL TRANSLATIONS: Information published in a foreign language considered to merit NASA distribution in English.

SPECIAL PUBLICATIONS: Information derived from or of value to NASA activities. Publications include conference proceedings, monographs, data compilations, handbooks, sourcebooks, and special bibliographies.

TECHNOLOGY UTILIZATION PUBLICATIONS: Information on technology used by NASA that may be of particular interest in commercial and other non-aerospace applications. Publications include Tech Briefs, Technology Utilization Reports and Notes, and Technology Surveys.

*Details on the availability of these publications may be obtained from:*

SCIENTIFIC AND TECHNICAL INFORMATION DIVISION

NATIONAL AERONAUTICS AND SPACE ADMINISTRATION

Washington, D.C. 20546